4D-Flow MRI of aortic and valvular disease

Juffermans, J.F.

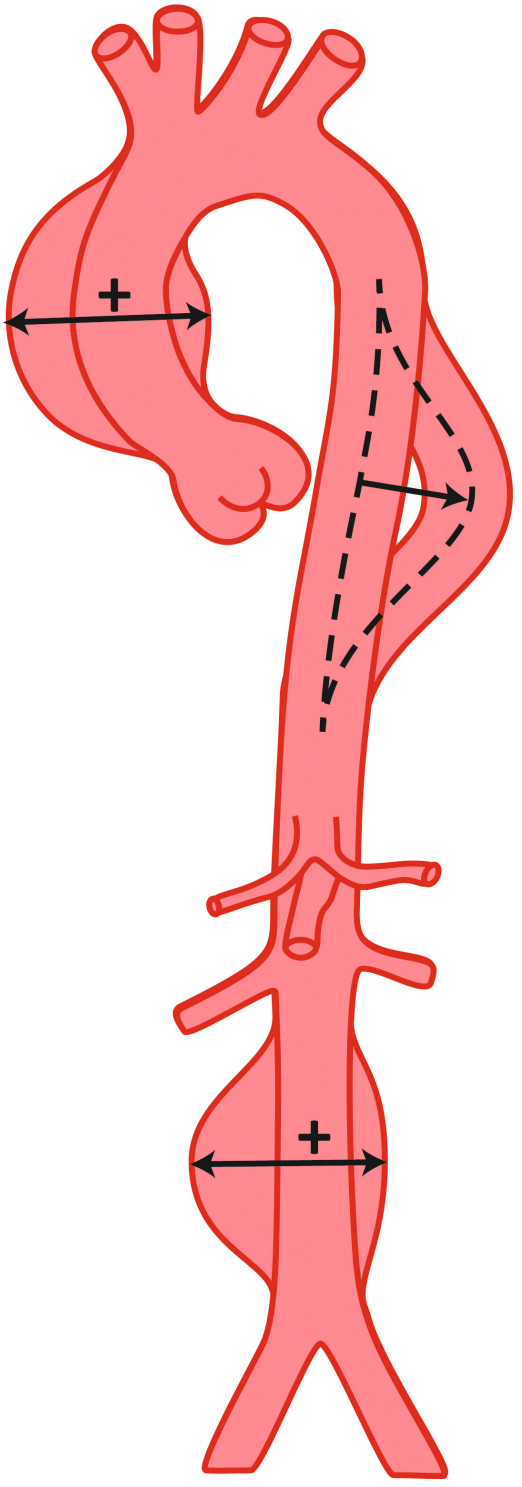

CHAPTER 5

Effects of Ageing on Aortic Hemodynamics Measured by 4D Flow MRI – A Case Series

Joe F. Juffermans, Jos J. M. Westenberg, Pieter J. van den Boogaard, and Hildo J. Lamb

EUROPEAN HEART JOURNAL–CASE REPORTS, 2023, YTAD130.

ABSTRACT

Background

It has been demonstrated that the rate of aortic dilatation is influenced by alteration of aortic hemodynamics, such as normalized flow displacement (FD_N) and wall shear stress (WSS). However, the effects of ageing and aortic diameter on aortic hemodynamics have not yet been described.

Case summary

4D-Flow MRI derived aorta hemodynamics were derived in the ascending aorta of a patient with ascending aortic aneurysm (mean ± standard deviation: 46 ± 1 mm) and a healthy volunteer (aortic diameter 30 ± 1 mm) with long-term follow-up of ten and eight years respectively. At all timepoints, compared to the healthy volunteer, the patient demonstrated higher magnitudes of FD_N (7% ± 1% versus 3% ± 1%) and WSS angle (36° ± 3° versus 24° ± 6°), and lower WSS magnitude (565 ± 100 mPa versus 910 ± 115 mPa), axial WSS (426 ± 71 mPa versus 800 ± 108 mPa) and circumferential WSS (297 ± 64 mPa versus 340 ± 85mPa). The patient and healthy volunteer demonstrated different aortic dilatation rates (regression slope ± standard error: 0.2 ± 0.1 versus 0.1 ± 0.2 mm per year) and trends in FD_N (0.1% ± 0.1% versus 0.1% ± 0.2% per year), WSS magnitude (22 ± 9 versus 35 ± 13 mPa per year), axial WSS (19 ± 4 versus 37 ± 7 mPa per year), circumferential WSS (9 ± 8 versus 5 ± 15 mPa per year), and WSS angle (-0.5 ± 0.4° versus -0.8° ± 1.0° per year).

Discussion

Aortic hemodynamic parameters are marginally affected by ageing and the aortic diameter in this case series. Since aortic hemodynamic parameters have been associated with aortic dilation by previous studies, the outcomes of the two subjects suggest that the aortic dilatation rate will remain constant while individuals are ageing and dilating.

INTRODUCTION

Aneurysms of the thoracic aorta are predominantly caused by degenerative disease and are mostly located in the ascending aorta [1, 2]. While thoracic aortic aneurysms (TAA) are mainly asymptomatic, the risk of aortic dissection, rupture or death increases significantly when the aortic diameter is larger than 60 mm [3]. Since the risk of these adverse events exceeds the risk of preemptive surgical aortic replacement [3], surgical repair is recommended for aortic diameters larger than 55mm for asymptomatic patients [1, 4]. While the yearly rates of aortic rupture, dissection or death is 14.1% for aortas with a diameter >60mm, adverse events are already considerable in aortas with diameters >50 mm or >40 mm as they have yearly rates of 6.5% and 5.3%, respectively [3]. Therefore, more comprehensive risk stratification methods for patients with TAA are needed [5]. It has been hypothesized (also referred as the "hemodynamic hypothesis") that the rate at which the aortic diameter increases is influenced by alterations in aortic hemodynamics which affect hemodynamic forces on the arterial wall [6]. The rate at which the aortic diameter increases is also known as the aortic dilatation rate.

Aortic hemodynamics can be assessed by 4D flow MRI which comprises a three dimensional velocity vector field over the cardiac cycle [7]. From the velocity vector field various parameters of aortic hemodynamics can mathematically be derived [8]. For the mathematical derivation of such parameters, a patient specific segmentation of the aortic lumen is required [9]. Although the resolution of the 4D flow MRI acquisition is not optimal, the shape of aortic lumen segmentation can be used to derive aortic morphology, like maximal aortic diameter and curvature radius [10, 11], especially when comparing for follow up. For some of the aortic hemodynamic parameters, it has already been demonstrated that they are associated with aortic dilatation rate, such as normalized flow displacement (FD_N; measure of flow eccentricity), regional elevated wall shear stress magnitude (WSS; viscous shear force on the vessel wall), circumferential WSS and WSS angle (angle between the axial and circumferential WSS) [6, 12-16]. Besides, the aortic diameter is well known to be inversely associated with the flow velocity and WSS [17]. So, presumably the aortic diameter, hemodynamics and dilatation rate are continuously influencing each other while ageing, see Figure 1. Since the long-term course of the aortic hemodynamics has not yet been reported, it is unknown if an increasing aortic diameter will change the aortic hemodynamics in such manner that the aortic dilatation rate will increase, decrease, or remains constant while ageing.

To review in this case series the natural course of aortic hemodynamics in individual subjects while ageing, we present a patient with an ascending aortic aneurysm and a healthy volunteer with a unique follow-up by 4D flow MRI of ten and eight years, respectively. To assess the variation and trend of the aortic diameters and 4D-flow MRI-derived hemodynamic parameters over all MRI examinations, the mean ± standard deviation and the regression slope ± standard error (SE) are quantified, respectively. The aortic diameter and hemodynamic parameters were quantified as previous described [10, 11].

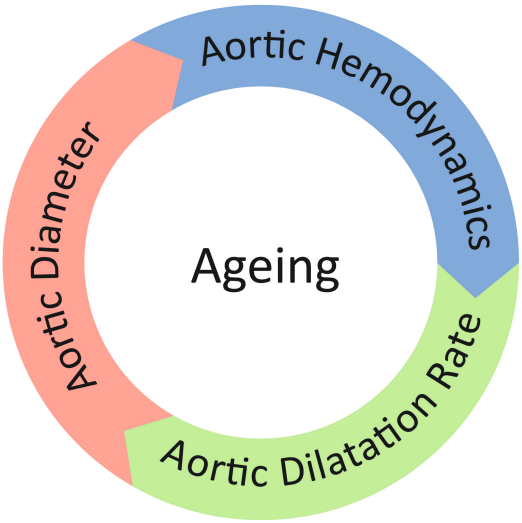

Figure 1. The potential coupling between the aortic diameter, hemodynamics and dilatation rate. These factors are possibly continuously influencing each other while ageing.

TIMELINE

Patient with Ascending Aortic Aneurysm						
Date	**Age [years]**	**MRI Examination**	**Aortic Diameter [mm]**	**FD_N [%]**	**Cir-WSS [mPa]**	**WSS angle [°]**
September 2012	52	1	44	6	185	35
April 2014	53	2	46	6	278	40
October 2017	57	3	45	7	375	39
January 2019	58	4	46	8	368	39
January 2021	60	5	46	7	290	33
June 2022	62	6	47	7	284	32
Healthy Volunteer						
Date	**Age [years]**	**MRI Examination**	**Aortic Diameter [mm]**	**FD_N [%]**	**Cir-WSS [mPa]**	**WSS angle [°]**
September 2014	45	1	29	2	279	25
March 2018	48	2	31	5	458	33
October 2019	50	3	30	3	220	17
December 2020	51	4	28	2	405	24
August 2020	53	5	31	4	338	20

Abbreviations: FD_N – normalized flow displacement, Cir-WSS – circumferential wall shear stress, and WSS – wall shear stress.

CASE SUMMARIES

Patient with Ascending Aortic Aneurysm

Over the course of 10 years a patient (male, 52–62 years, 77–81 kg, 187 cm, body surface area (BSA) 1.93–2.06 m^2, Caucasian) with ascending aortic aneurysm of the outpatient clinic of the Leiden University Medical Center underwent serial MRI examinations for disease surveillance, which included 4D flow MRI of the thoracic aorta. Other than the aortic aneurysm, there are no other diseases known to the patient. A decade after his first MRI examination, the asymptomatic patient underwent his sixth and most recent 4D flow MRI examination, see Figure 2. For details about the MRI system and 4D flow MRI sequences see Table 1. The aortic diameter and hemodynamic parameters of the ascending aorta were calculated at peak systole for all examination and are summarized in Table 2.

At the first (September 2012) and last (June 2022) 4D flow MRI examination, the maximal diameter of the ascending aorta measured 44 and 47 mm, respectively. While using the outcomes of all six 4D flow MRI acquisitions, the average maximal diameter ± standard deviation of the ascending aorta was 46 ± 1 mm and regression slope ± standard error (SE) showed an average increase of 0.2 ± 0.1 mm per year. The average aortic diameter indexed for BSA was 2.31 cm/m^2 [18].

Furthermore, the mean blood velocity in the ascending aorta was 37 ± 2 cm/s at peak systole and the regression slope showed a decrease close to the SE over time (-0.2 ± 0.2 cm/s per year). Mean FD_N was 7% ± 1% and the regression slope showed an increase close to the SE over time (0.1% ± 0.1 % per year). The mean WSS magnitude, and its axial and circumferential component, were 565 ± 100, 426 ± 71 and 297 ± 64 mPa, respectively. Mean WSS magnitude and axial WSS increased on average (22 ± 9 and 19 ± 4 mPa per year, respectively) while the regression slope of circumferential WSS showed no change relative to the SE over time (9 ± 8 mPa per year). The mean WSS angle was 36° ± 3° and decreased on average with -0.5° ± 0.4° per year.

The aortic hemodynamics per MRI acquisition are illustrated in Figure 3 by radial-plots. This figure demonstrates comparable hemodynamic patterns between the follow-up examinations for the patient. This agreement in aortic hemodynamics between the follow-up examinations is also demonstrated by the relatively small standard deviations of the parameters.

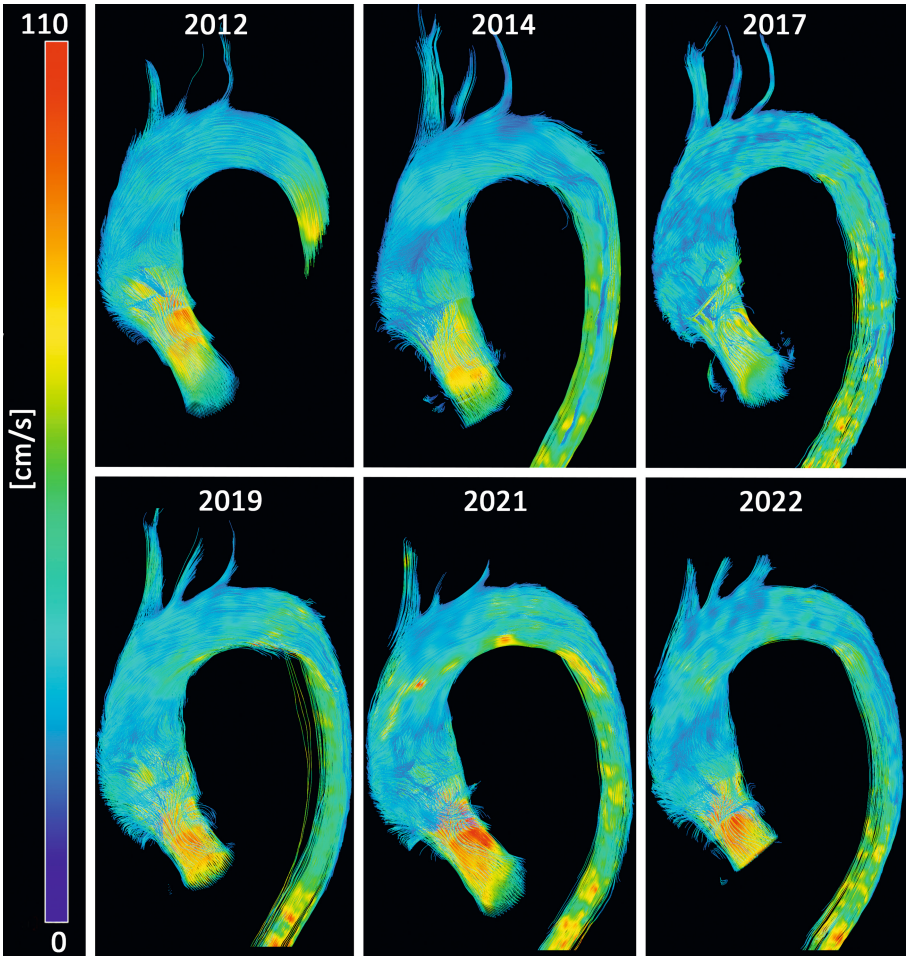

Figure 2. Peak systolic streamline visualizations of the 4D flow MRI acquisitions of a patient with an ascending aortic aneurysm.

Table 1. Details of the MRI Scanner and 4D Flow MRI Sequence.

Characteristics	**Patient**					
year	**2012**	**2014**	**2017**	**2019**	**2021**	**2022**
Vendor Philips Healthcare						
Type	NT 15 Gyroscan Intera	Ingenia			Ingenia Elition	
Field strength [T]	1.5	3				
Field of View [mm^3]	480 x 240 x 90	400 x 300 x 60	350 x 250 x 70	350 x 300 x 75	350 x 270 x 84	350 x 290 x 75
Acquired Isotropic Spatial Resolution [mm^3]	5.0	2.5			3.0	2.5
Reconstructed spatial resolution [mm^3]	1.9 x 1.9 x 5.0	2.5 x 2.5 x 2.5	1.5 x 1.5 x 2.5	1.8 x 1.8 x 2.5	1.5 x 1.5 x 3.0	1.5 x 1.5 x 2.5
Reconstructed temporal resolution [ms]	35	50	30	34	33	42
Reconstructed phases [n]	30	24	40	32	32	32
Echo time [ms]	3.9	3.2	2.3	2.7	2.7	2.7
Repetition time [ms]	6.7	6.0	4.2	4.6	4.6	4.6
Flip Angle [degrees]	10					
Readout method	Cartesian					
Number of signal average	2	1				
Acceleration Method	EPI: 5	SENSE: 2.0 x 1.0*	TFE: 2 SENSE: 2.5 x 1.5*	TFE: 2 SENSE: 2.5 x 1.2*		
Cardiac gating	Retrospective					
Hemi-diaphragm respiratory navigator gating	No	Yes				
Flow-encoding scheme	Asymmetric four-point					
VENC [cm·s]	150	200	200	150	150	150

Table 1. *Continued*

Characteristics	**Healthy Volunteer**				
year	**2014**	**2018**	**2019**	**2020**	**2022**
	Vendor Philips Healthcare				
Type	Ingenia	Ingenia Elition	Ingenia	Ingenia Elition	
Field strength [T]	3				
Field of View [mm^3]	400 x 350 x 60	350 x 260 x 70	350 x 270 x 70	400 x 260 x 60	320 x 280 x 60
Acquired Isotropic Spatial Resolution [mm^3]	2.5		3.0	2.5	
Reconstructed spatial resolution [mm^3]	2.5 x 2.5 x 2.5	1.5 x 1.5 x 2.5	1.5 x 1.5 x 3.0	1.3 x 1.3 x 2.5	1.4 x 1.4 x 2.5
Reconstructed temporal resolution [ms]	47	34	34	29	36
Reconstructed phases [n]	21	30	32	34	32
Echo time [ms]	3.2	2.6	2.5	2.7	2.6
Repetition time [ms]	6.0	4.5	4.3	4.6	4.5
Flip Angle [degrees]	10				
Readout method	Cartesian				
Number of signal average	1				
Acceleration Method	SENSE: 2.0 x 1.0*	TFE: 2 SENSE: 2.5 x 1.5*		TFE: 2 SENSE: 2.5 x 1.2*	
Cardiac gating	Retrospective				
Hemi-diaphragm respiratory navigator gating	Yes				
Flow-encoding scheme	Asymmetric four-point				
VENC [cm·s]	200	200	175	150	175

Abbreviations: VENC – velocity encoding , EPI – echo-planar imaging, SENSE – sensitivity encoding, and TFE – turbo field echo. * – in-plane and out-of-plane parallel reduction factor, respectively.

Table 2. Morphology and Hemodynamics of Ascending Aorta at Peak Systole.

Patient								
Year	**2012**	**2014**	**2017**	**2019**	**2021**	**2022**	**Mean ± SD**	**β ± SE**
Age	52	53	57	58	60	62	57 ± 4	
Maximal Diameter [mm]	44	46	45	46	46	47	46 ± 1	0.2 ± 0.1
Flow Velocity [cm/s]	38	36	37	39	37	33	37 ± 2	-0.2 ± 0.2
Normalized Flow Displacement [%]	6	6	7	8	7	7	7 ± 1	0.1 ± 0.1
WSS magnitude [mPa]	379	493	656	659	598	604	565 ± 100	22 ± 9
Axial WSS [mPa]	301	356	466	485	470	479	426 ± 71	19 ± 4
Circumferential WSS [mPa]	185	278	375	368	290	284	297 ± 64	9 ± 8
WSS angle [°]	35	40	39	39	33	32	36 ± 3	-0.5 ± 0.4
Healthy Volunteer								
Year	**2014**		**2018**	**2019**	**2020**	**2022**	**Mean ± SD**	**β ± SE**
Age	45		48	50	51	53	50 ± 3	
Maximal Diameter [mm]	29		31	30	28	31	30 ± 1	0.1 ± 0.2
Flow Velocity [cm/s]	56		49	51	56	58	54 ± 4	0.3 ± 0.7
Normalized Flow Displacement [%]	2		5	3	2	4	3 ± 1	0.1 ± 0.2
WSS magnitude [mPa]	731		952	824	1,008	1,035	910 ± 115	35 ± 13
Axial WSS [mPa]	642		756	763	892	948	800 ± 108	37 ± 7
Circumferential WSS [mPa]	279		458	220	405	338	340 ± 85	5 ± 17
WSS angle [°]	25		33	17	24	20	24 ± 6	-0.8 ± 1.0

Abbreviations: SD – standard deviation, β – beta (i.e., the difference per year) of the regression analysis, SE – standard error (SE)

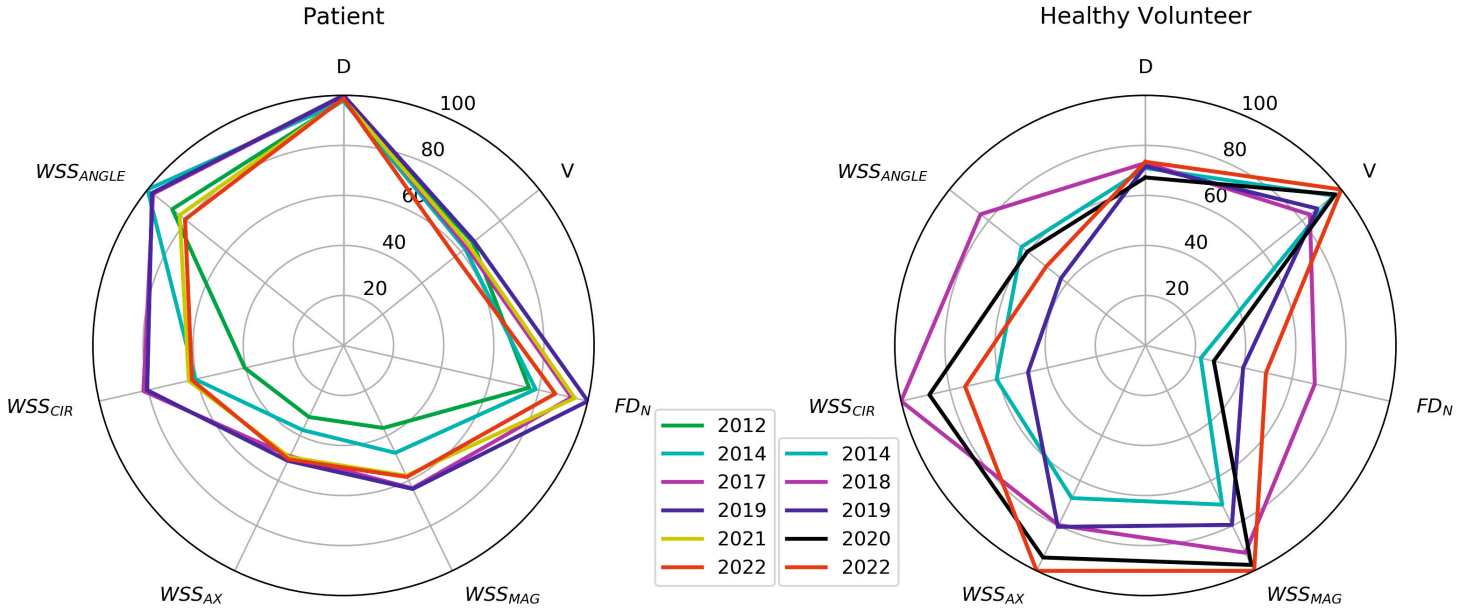

Figure 3. Radial-plots of hemodynamic parameters obtained from the 4D flow MRI acquisitions of the patient (left) and healthy volunteer (right). In order to compare hemodynamic parameters, the magnitudes were indexed to highest magnitude among all MRI examinations and both subjects and presented as percentage. Abbreviations; D – diameter, V – flow velocity, FD_N – normalized flow displacement, WSS_{MAG} – wall shear stress magnitude, WSS_{AX} – axial wall shear stress, WSS_{CIR} – circumferential wall shear stress, and WSS_{ANGLE} – wall shear stress angle.

Healthy Volunteer

Over the course of eight years a healthy volunteer (male, 45–53 years, 70–73 kg, 180 cm, BSA 1.89–1.92 m^2, Caucasian) underwent five MRI examinations for scientific research including a 4D flow acquisition of the thoracic aorta, see Figure 4. For details about the MRI scanner and sequences see Table 1. The aortic diameter and hemodynamic parameters of the ascending aorta were measured at peak systole and are summarized in Table 2.

At the first (September 2014) and last (August 2022) 4D flow MRI examination, the maximal diameter of the ascending aorta measured 29 and 31 mm, respectively. While using the outcomes of all five examinations, the average maximal diameter of the ascending aorta was 30 ± 1 mm and the regression slope showed no change relatively to the SE (0.1 ± 0.2 mm per year). The average aortic size indexed for BSA was 1.57 cm/m^2 [18].

Besides, the mean blood velocity in the ascending aorta was 54 ± 4 cm/s at peak systole and regression slope showed no change relative to the SE over time (0.3 ± 0.7 cm/s per year). Mean FD_N was 3% ± 1% and the regression slope showed no change relative to the SE over time (0.1% ± 0.2% per year). The mean WSS magnitude, and its axial and circumferential component, were 910 ± 115, 800 ± 108 and 340 ± 85 mPa, respectively. Mean WSS magnitude and axial WSS increased on average (35 ± 13 and 37 ± 7 mPa per year, respectively) while circumferential WSS showed no change relative to the SE over time (5 ± 17 mPa per year). The mean WSS angle was 24° ± 6° and the regression slope showed no change relative to the SE over time (-0.8 ± 1.0° per year).

DISCUSSION

The normal increase in aortic diameter per decade of an ageing aorta without aneurysm is 0.9 mm in men and 0.7 mm in women [4]. Besides an aortic diameter >55 mm, asymptomatic patients with high dilatation rates (>3 – 5 mm per year) should be considered for surgical replacement [1, 4]. In this case series one patient with ascending aneurysm and one healthy volunteer were presented with a unique follow-up by 4D flow MRI of ten and eight years, respectively. The patient showed an aortic dilatation rate of 0.2 ± 0.1 mm per year (i.e., 2 ± 1 mm per decade) which is considerably higher than the aortic dilatation rate of an ageing aorta without aneurysm.

When the aortic hemodynamics of the subjects in this case series are compared, the patient demonstrated higher magnitudes of normalized flow displacement (7% ± 1% versus 3% ± 1%) and WSS angle (36° ± 3° versus 24° ± 6°) but lower flow velocity (37 ± 2 cm/s versus 54 ± 4 cm/s), WSS magnitude (565 ± 100 mPa versus 910 ± 115 mPa), axial WSS (426±71 mPa versus 800 ± 108 mPa) and circumferential WSS (297 ± 64 mPa versus 340 ± 85mPa) as compared to the healthy volunteer.

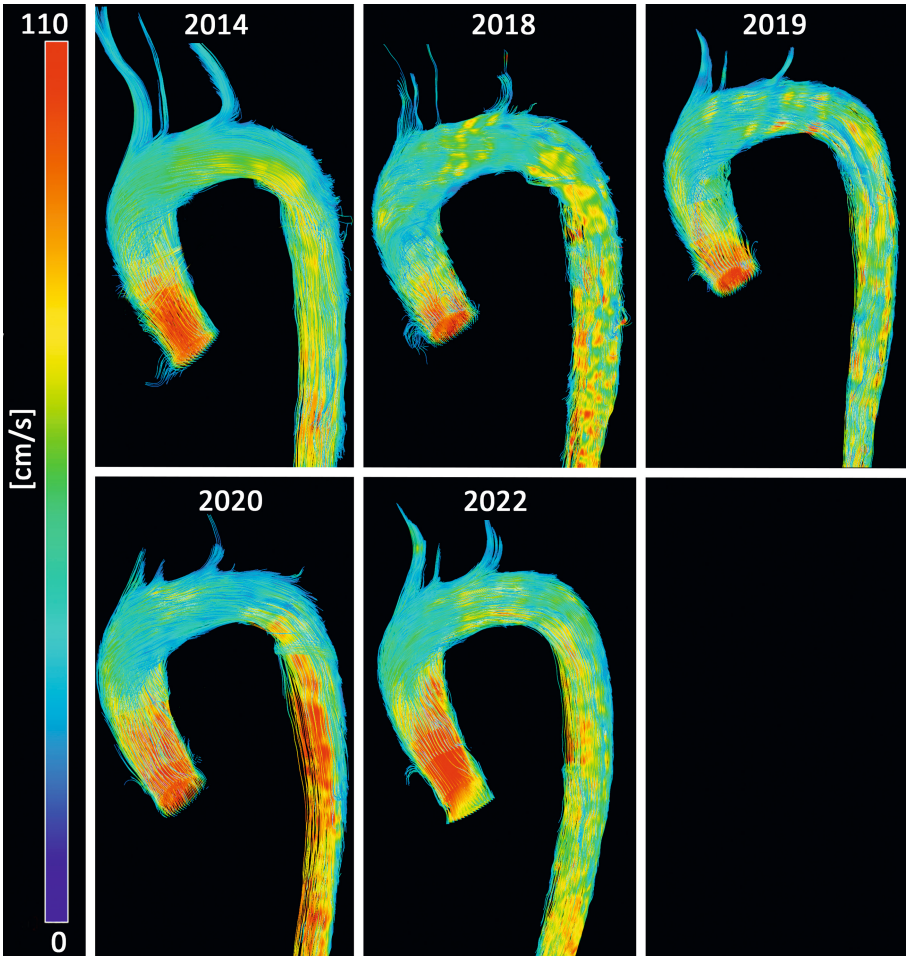

Figure 4. Peak systolic streamline visualizations of the 4D flow MRI acquisitions of a healthy volunteer.

Previous studies have demonstrated that increased magnitudes of FDN, circumferential WSS and WSS angle are associated with higher aortic dilatation rates [12-16]. Based upon these previous studies, the higher aortic dilatation rate of the patient could be explained by the observed magnitudes of FDN and WSS angle but not circumferential WSS.

While the maximal diameter of the healthy volunteer in this case series showed no change relative to the SE during the follow-up (0.1 ± 0.2 mm per year), the mean flow velocity, FDN, circumferential WSS and WSS angle also showed no change relative to the SE over time. However, the WSS magnitude and axial WSS showed increase over time (35 ± 13 and 37 ± 7 mPa per year, respectively). These outcomes suggest that, at least for the healthy volunteer in this case series over a follow-up period of 8 years,

aortic hemodynamic parameters are probably only marginally affected by ageing in aortas with normal diameters.

In contrast, the ascending aorta of the patient demonstrated a considerable aortic dilatation rate during follow-up. While mean flow velocity decreased close to the SE over time (-0.2 ± 0.2 cm/s per year), the mean WSS magnitude and axial WSS both showed increase (22 ± 9 and 19 ± 4 mPa per year, respectively). The circumferential WSS and FDN showed no change relatively to the SE. The more predominant increase of axial WSS compared to circumferential WSS presumably explains the decrease in WSS angle (-0.5° ± 0.4° per year). These outcomes suggest that, at least for the patient in this case series over a follow-up period of 10 years, aortic hemodynamic parameters are probably only marginally affected by ageing and the aortic diameter in thoracic aortic aneurysm. Since aortic hemodynamic parameters have been associated with aortic dilation by previous studies [12-16], we expect that the dilatation rate will remain approximately constant in patients with thoracic aortic aneurysm while these patients are ageing and dilating. In other words, the increase in aortic diameter will presumably not affect the aortic hemodynamics of patients in such manner that the aortic dilatation rate will further increase or decrease. This pathophysiological mechanism of thoracic aortic aneurysms possibly explains the growth of the aneurysm in some patients.

In addition, the flow velocity and the WSS magnitude are both well known to be inversely associated with the vessel diameter [17]. This coupling between the aortic diameter and flow velocity will affect the magnitude of several hemodynamic parameters which are mathematically derived from the velocity vectors [8]. Hereby, the hemodynamic parameters, which are affected by the inverse association between aortic diameter and flow velocity, indirectly will reflect the aortic dilation. In contrast, the FDN and WSS angle describe the eccentricity and asymmetry of the flow profile independent of the flow velocity and vessel diameter, respectively [16, 19]. We hypothesize that hemodynamic parameters, which are not affected by the inverse association between aortic diameter and flow velocity, will demonstrate a stronger association with the aortic dilatation rate and risk stratification of patients with TAA.

The unlikely negative dilatation rates between some MRI acquisitions of the patient and healthy volunteer demonstrate the measurement uncertainty of aortic diameters. Like all parameters assessed by an imaging modality, the precision and accuracy of the quantification of the maximal vessel diameter is affected, among other factors, by the imaging modality, acquisition, quantification method, and observer variability [8, 11, 20]. As a result, a clinical guideline indicated that changes in maximal diameter <3 mm could not reliable be detected [4]. Based upon the aortic dilatation rate of an ageing aorta without aneurysm, reliable differences in the aortic diameter of healthy volunteers can presumably be measured after 3.3 decades (3/0.9 mm per decade) in men and 4.3 decades (3/0.7 mm per decade) in women. Besides, the relatively large standard

errors of the regression analyses compared to the regression slopes demonstrates the uncertainties while estimating the trends of most quantified parameters.

The patient and healthy volunteer demonstrated approximately comparable levels of variation for the hemodynamic parameters between follow-up examinations. This overlap in variation demonstrates the robustness of 4D flow MRI to capture aortic hemodynamics, despite of variation in MRI scanners and 4D flow sequences. While no unexpected changes in the aortic hemodynamics were observed between MRI examinations, variation in MRI scanners and 4D flow sequences potentially may affect quantified parameters. The aortic diameters indexed for BSA of the patient and healthy volunteers both are associated with a low risk for complications (i.e., ±1% per year) [18]. Patients with an increased risk for complications could possibly demonstrate different trends in aortic hemodynamics while ageing and dilatation.

CONCLUSION

Aortic hemodynamic parameters are marginally affected by ageing and the aortic diameter in this case series. Since aortic hemodynamic parameters have been associated with aortic dilation by previous studies, the outcomes of the two subjects suggest that the aortic dilatation rate will remain constant while individuals are ageing and dilating.

REFERENCES

1. Members, W.C., et al., 2022 ACC/AHA guideline for the diagnosis and management of aortic disease: a report of the American Heart Association/American College of Cardiology Joint Committee on Clinical Practice Guidelines. Journal of the American College of Cardiology, 2022.
2. e Melo, R.G., et al. Incidence and prevalence of thoracic aortic aneurysms: A systematic review and meta-analysis of population-based studies. in Seminars in Thoracic and Cardiovascular Surgery. 2021. Elsevier.
3. Elefteriades, J.A., Natural history of thoracic aortic aneurysms: indications for surgery, and surgical versus nonsurgical risks. The Annals of thoracic surgery, 2002. **74**(5): p. S1877-S1880.
4. Erbel, R., et al., 2014 ESC Guidelines on the diagnosis and treatment of aortic diseases: Document covering acute and chronic aortic diseases of the thoracic and abdominal aorta of the adult The Task Force for the Diagnosis and Treatment of Aortic Diseases of the European Society of Cardiology (ESC). European heart journal, 2014. **35**(41): p. 2873-2926.
5. Pape, L.A., et al., Aortic diameter≥ 5.5 cm is not a good predictor of type A aortic dissection: observations from the International Registry of Acute Aortic Dissection (IRAD). Circulation, 2007. **116**(10): p. 1120-1127.
6. Soulat, G., et al., Association of regional wall shear stress and progressive ascending aorta dilation in bicuspid aortic valve. JACC: Cardiovascular Imaging, 2022. **15**(1): p. 33-42.
7. Markl, M., et al., Time-resolved three-dimensional phase-contrast MRI. Journal of Magnetic Resonance Imaging: An Official Journal of the International Society for Magnetic Resonance in Medicine, 2003. **17**(4): p. 499-506.
8. Soulat, G., P. McCarthy, and M. Markl, 4D Flow with MRI. Annual Review of Biomedical Engineering, 2020. **22**: p. 103-126.
9. Dyverfeldt, P., et al., 4D flow cardiovascular magnetic resonance consensus statement. Journal of Cardiovascular Magnetic Resonance, 2015. **17**(1): p. 72.
10. Juffermans, J.F., et al., Reproducibility of aorta segmentation on 4D flow MRI in healthy volunteers. Journal of Magnetic Resonance Imaging, 2020.
11. Juffermans, J.F., et al., 4D Flow MRI in Ascending Aortic Aneurysms: Reproducibility of Hemodynamic Parameters. Applied Sciences, 2022. **12**(8): p. 3912.
12. van Hout, M., et al., Ascending aorta curvature and flow displacement are associated with accelerated aortic growth at long-term follow-up: A MRI study in Marfan and thoracic aortic aneurysm patients. IJC Heart & Vasculature, 2022. **38**: p. 100926.
13. Korpela, T., et al., Flow displacement and decreased wall shear stress might be associated with the growth rate of an ascending aortic dilatation. European Journal of Cardio-Thoracic Surgery, 2022. **61**(2): p. 395-402.
14. Hope, M.D., et al., MRI hemodynamic markers of progressive bicuspid aortic valve-related aortic disease. Journal of Magnetic Resonance Imaging, 2014. **40**(1): p. 140-145.
15. Guala, A., et al., Wall shear stress predicts aortic dilation in patients with bicuspid aortic valve. JACC: Cardiovascular Imaging, 2021.
16. Minderhoud, S., et al., Wall shear stress angle determines aortic growth in patients with bicuspid aortic valves. European Heart Journal-Cardiovascular Imaging, 2021. **22**(Supplement_2): p. jeab090. 120.
17. Callaghan, F.M. and S.M. Grieve, Normal patterns of thoracic aortic wall shear stress measured using 4D-flow MRI in a large population. American Journal of Physiology-Heart and Circulatory Physiology, 2018.

18. Davies, R.R., et al., Novel measurement of relative aortic size predicts rupture of thoracic aortic aneurysms. The Annals of thoracic surgery, 2006. **81**(1): p. 169-177.
19. Sigovan, M., et al., Comparison of four-dimensional flow parameters for quantification of flow eccentricity in the ascending aorta. Journal of Magnetic Resonance Imaging, 2011. **34**(5): p. 1226-1230.
20. Elefteriades, J.A. and E.A. Farkas, Thoracic aortic aneurysm clinically pertinent controversies and uncertainties. J Am Coll Cardiol, 2010. **55**(9): p. 841-57.